International Journal of Latest Trends in Engineering and Technology
Vol.(10)Issue(1), pp.113-120
DOI: http://dx.doi.org/10.21172/1.101.18
e-ISSN:2278-621X

EFFECT OF HNO3 AND CL¯ ON CORROSION BEHAVIOUR OF CR-MN AUSTENITIC STAINLESS STEELS

Nilay N. Khobragade[1], Awanikumar P. Patil[2]

Abstract- Due to rising cost of Ni, there is interest in low cost Ni-free (Cr-Mn) austenitic stainless steels for a few industrial applications. The present work deals with studying effect of HNO_3/Cl^- ratio on corrosion behaviour of Cr-Mn austenitic stainless steel (Cr-Mn ASS). Test methods used were potentiodynamic polarisation (PDP), electrochemical impedance spectroscopy (EIS) and Mott-Schottky analysis. Test solutions were 1000 ppm Cl^-, 0.01M HNO_3+1000 ppm Cl^-, 0.1M HNO_3+1000 ppm Cl^- and 1M HNO_3+ 1000 ppm Cl^-. From PDP plots it was found Cr-Mn ASS exhibited active corrosion in 1000 ppm Cl^- and passivity in HNO_3 containing test solutions. From EIS results it was found that polarisation resistance (Rp) decreased on addition of HNO_3 for the both the test steel. This is attributed to effect of pH on stability of Cr_2O_3 film. The film of Cr_2O_3 is a p-type semiconductor and has vacancies in cation sub-lattice. When Cl^- is incorporated in anion sub-lattice in sets in Schottky pair reaction by which anion vacancies are created. These vacancies allow migration of cations from metal-film interface to film-solution interface and anions in reverse direction by vacancy aided diffusion process. Therefore, the film forming on test alloys were characterised by Mott-Schottky analysis to find out cation and anion defect densities of passivating film in 1000 ppm Cl^- and 0.1M HNO_3+1000 ppm Cl^- solutions. It was found that density of the cation vacancies in the film forming on Cr-Mn ASS in 1000 ppm Cl^- solution was 12.6 $x10^{20}$ per cm^3, and increased to 87.5 $x10^{20}$ per cm^3 on addition of HNO_3. This explains the role of HNO_3 addition. It was also found that the density of oxygen (anion) vacancies for the test steel was 13$x10^{20}$ per cm^3 in 1000 ppm Cl^- solution and increased to 29.6$x10^{20}$ per cm^3 for Cr-Mn ASS. The rise in defect densities is attributed to drop in pH on addition of HNO_3.
Keywords: Cr-Mn-Ni Austenitic Steels, Nitric Acid, Chloride, Corrosion

1. INTRODUCTION

Austenitic stainless steel (e.g. 304 SS in 300 series of austenitic stainless steel) is standard construction material for many industrial applications owing to its excellent corrosion resistance, mechanical strength and good weldability [1]. However, due to rising costs of Ni, interest in low-Ni or Ni-free austenitic stainless steels (Cr-Mn-Ni ASS or Cr-Mn ASS) is increasing [2]. These steels in general are termed as 200 series ASS and account for more than 10% of total stainless steel production [3]. It is expected that their demand would grow with rising cost of Ni. However, due to various reasons, properties of these grades are inferior to well established grades of 300 series. For example, in absence of Ni, austenitic structure is ensured by 6-10% Mn together with N and/or Cu in 200 series grades or Ni-free Cr-Mn grades [4]. But reducing Ni, limits the maximum Cr-content possible in the alloy and therefore, Cr-content of the 200-series alloys is lower than 300 series alloys. The stainless steels accrue their excellent corrosion resistance primarily from a thin and compact film of Cr_2O_3, which passivates these alloys [1]. Extent of passivation depends upon Cr content and therefore, SS alloys with relatively lower Cr-content will naturally, have lower corrosion resistance. Secondly, Ni not only increases formability, weldability and toughness, but also improves corrosion resistance [5]. It is well known that N addition helps improving corrosion resistance of stainless steel alloys [6]. However, there have been cases of false claim about chemical composition of Cr-Mn ASS. Therefore, chemical composition of 200 grades or Ni-free Cr-Mn steels is suspected and it is recommended that such steels are sourced from highly reputable and informed suppliers [3]. However, when there is increasing pressure to cut cost, it is natural to develop proprietary Cr-Mn SS alloys, not covered by standard chemical specifications. All such new grades obviously have not yet been studied for their corrosion behaviour. Since Ni reserves are rather limited, it is important to investigate performance of Ni-free Cr-Mn ASS thoroughly. So that the end users have sufficient information about properties of newer stainless steels in general and Ni-free/ low Ni Cr-Mn alloys in particular.

1.1 Pitting Corrosion

Pitting corrosion following breakdown of passive film is one of the most dangerous forms of local attack for steels especially in chloride media. Regarding the relationship between pitting potential, E_{pit}, and chloride concentration, $[Cl^-]$, it has been shown [7] that for type 304 SS a linear dependence exists of the type (Eq. 1.1)

$$E_{pit} = A + B \log [Cl^-] \qquad (1.1)$$

where, A and B are constants.

[1] Assistant Professor, Department of Metallurgical Engineering, Government College of Engineering, Amravati, India
[2] Professor, Department of Metallurgical and Materials Engineering, Visvesvaraya National Institute of Technology, Nagpur, India

The major efforts to prevent this type of attack were undertaken by metallurgists in developing new alloys highly resistant to chloride environments. It is often stated that the pitting corrosion resistance of stainless steels depends mainly upon the chromium, molybdenum, and nitrogen content. One method of estimating the pitting resistance equivalent number (PREN) is as follows (Eq. 1.2):

$$PREN = (\%Cr) + 3 \times (\%Mo) + 15 \times (\%N) \quad (1.2)$$

The major disadvantage of these new alloys is their high cost compared with conventional stainless steels, due to the higher percentage of the alloying elements such as Cr, Ni and Mo, as well as the complexity of the fabrication process. The favorable effect of these alloying elements on the pitting resistance is attributed either to the formation of a protective passive surface film containing these elements, or to the adsorption of soluble products of these elements (e.g., MoO_4^{2-} in case of alloyed Mo) [8]. These assumptions have been confirmed by experiments [9]. An attempt has been made to minimize the amounts of expensive alloying elements like Mo or W, by ionic implantation in the superficial layers of alloys. However, implantation causes structural changes, like the austenite-ferrite transformations, resulting in an increase of pit density on the transformed areas. Electrochemical incorporation, from a solution containing molybdate, in the outer part of the passive film, therefore appears a sufficient and non-disturbing method to ensure a protective character to the passive layer. This process was successfully applied on titanium, aluminum, and steel. Molybdenum was shown to improve the corrosion resistance when incorporated in the passive layer [10].

1.2 Inhibitors

Kim et al have used X-ray photoelectron spectroscopy (XPS) to study effect of nitrate on passive film of 304SS and found presence of surface nitride [11]. It is explained that nitride is produced by reduction of NO_3 , and enhances pitting resistance of 304 SS because the nitride acts as (i) precursor to the passive oxide film and (ii) a buffer to local acidity, which stabilizes the layers of passive film. Identical surface nitride is present on N alloyed 304 SS, when these steels are anodically polarized in 0.1 M HCl. It indicates that nitrate reduction produces surface nitride; it can also be produced by adding nitrogen in SS. As such, increasing the nitrogen in 316LN SS, increases nitrate in the passive film [12]. Presence of nitrate in the passive film improves the pitting corrosion resistance [17]. However**,** it has been found that beyond critical concentration of N, the corrosion rate increases [13].

Corrosion behaviour of any material is determined by nature of passive film and its interaction with the environment; therefore it is essential to investigate how the passivity develops and deteriorates under different environmental conditions. The important environmental factors are solution concentration (presence of aggressive anion such as chloride or presence of inhibitors such as nitrates, molybdates) and pH.

Therefore, in this investigation, the effect of inhibitors on stainless steel is studied so as to predict the possible corrosion properties as if it is alloyed with various alloying elements. The elements are chosen according to number, pitting resistance equivalent number (PREN) such as Mo and N. The effect of inhibitors on stainless steel is studied in Cl^- free and Cl^- containing solutions. Also, the effect of pH was investigated to study its influence on electrochemical, electronic and semi conducting properties of passive films of ASS.

2 EXPERIMENTAL WORK

The present investigation involves the study of Chrome-Manganese austenitic stainless steel (Cr-Mn ASS). Cr-Mn ASS was procured from the market in the form of sheets (3 mm thick). Specimens of 10 mm x 10 mm size were cut by using electrolytic discharge cutting machine (EDM) from these sheets. Initially to homogenize the microstructure, specimens were solution annealed in silicon carbide muffle furnace (Lenton make) at $1050^0C \pm 2^0C$ for one hour and then quenched in water. Chemical composition of these steels is given in Table 1.

Table 1: Chemical composition of studied Cr-Mn ASS austenitic stainless steel in weight %.

Elements	C	Cr	Ni	Mn	Si	P	S	Fe
Cr-Mn ASS	0.11	15.86	0.31	9.60	0.434	0.0678	0.0041	Bal.

2.1 Specimen preparation

For electrochemical tests, a piece of copper strip (0.8 mm X 0.8 mm X 3 mm) was soldered with single strand insulated copper wire (18 gauge), then the copper strip was pasted by conducting silver paste on SS specimens and then mounted in araldite to embed the soldered joint leaving other face of specimen open. The open face of specimen was then abraded on series of emery paper (120-800 grit) and then polished on a cloth smeared with 0.75 µm alumina. The specimen was ultrasonically cleaned after every stage and then used in tests.

2.2 Electrochemical tests

Electrochemical tests were carried out in standard 3-electrode system contained in 600 ml four-neck round bottom corning flask; saturated calomel electrode (SCE) was reference electrode and cylindrical platinum gauze electrode was counter electrode. A computer controlled Potentiostat (VersaSTAT 3 of EG&G PAR) was used in conjunction with its V3-Studio software (Princeton Applied Research). The software runs and controls the test, acquires data during the test and saves it.

2.2.1 OCP measurement (Time-potential studies)
After setting up the cell, the specimens were subjected to cathodic cleaning at -1V (SCE) for 1 minute, then left to achieve stable open circuit potential (OCP) for 30 minutes, during which the OCP was recorded and then plotted.

2.2.2 Electrochemical impedance spectroscopy
After time-potential measurement, EIS experiment was conducted by using a sinusoidal AC signal of 10 mV in a frequency range of 10^{5} to 10^{-2} Hz at open circuit potential. These experiments were controlled by standard V3 Studio software. The results were then plotted in the form of Z'-Z" plots (Nyquist plots) for various test environments.

2.2.3 Anodic polarization
Soon after EIS test was over, polarization test was started from a cathodic potential (OCP minus 300 mV (SCE) and continued up to an anodic potential of 1.5V (SCE). The polarization experiment was carried out at the scan rate of 10mV/min. Electrochemical tests were conducted for triplicate specimens in each experimental condition and all the results obtained were reproducible. Polarization plots were then used to get various electrochemical data. Tafel slopes βa (mV) and βc (mV) and the i_{corr} (μA/cm^2) and were obtained by employing Tafel extrapolation on anodic and cathodic parts of these plots simultaneously using CorrView (Version 2.9) software (Scribner Associates Inc.). The results were then plotted in the form of E- log (i) plots.

2.2.4 Equivalent circuits
The EIS results were interpreted using an 'equivalent circuit' (Figure 1) based on electrochemical-physical model to represent electrochemical interface. This circuit consists of electrical elements [Rs (CPE‖pR)], where Rs is solution resistance, CPE is constant phase element in parallel connection with Rp, which is polarization resistance at the interface. This circuit was chosen to minimize circuit element and to fit experimental data reasonably by keeping error value less than 10%. The electrical parameter values of these circuit elements were obtained directly by fitting the experimental impedance plots with the help of Zview Version-2 (Scribner Inc.) software. In these EIS experiments, CPE is used to obtain better fit for experimental data, represents the capacitance of the passive oxide layer. The impedance expression of CPE is given as (Eq. 2.1)

$$Z_{CPE} = 1 / [T (I*w)^{P}], \quad (2.1)$$

where, w is the angular frequency, T and P are frequency dependent fit parameters,
$I = (-1)^{1/2}$ and $w = 2\pi f$, where f is frequency (Hz).

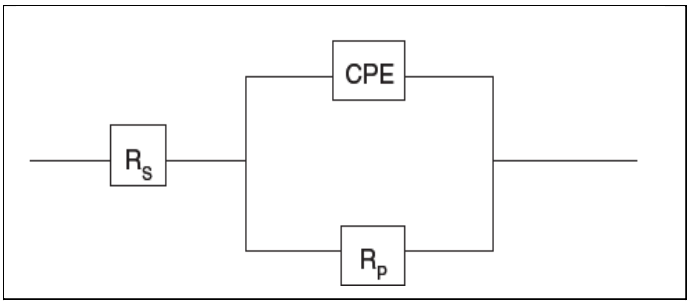

Figure 1: The equivalent circuit used for fitting of impedance data

2.2.5 Mott-Schottky analysis
Mott-Schottky (M-S) analysis was performed by measuring capacitance immediately after EIS measurements. The capacitance measurements were made on specimens to understand the semiconducting property of the passive film. The polarization cell was used with platinum mesh as a counter electrode and saturated calomel as a reference electrode. VersaSTAT 3 (PAR) FRA was used for these measurements. The films formed on test steels at OCP in various environments were chosen for M-S analysis. The specimens were exposed for four hours to the solution prior to capacitance measurements at OCP. M-S analysis was done for the solution conditions presented in Table 2.

Table 2: Test matrix of solution chemistry and its conditions for Mott-Schottky analysis.

Sl. No.	Concentration of solution	Cl^- concentration , ppm
2	DD water	1000
3	0.1 M HNO_3	1000

The capacitive measurements were carried out at a constant frequency of 1000 Hz at 10 mV amplitude voltage as a function of applied potential by potentiodynamic sweeping from -1.5 (SCE) to +1.5V (SCE) at the sweep rate of 10 mV/s. The capacitance (C) was calculated using the Eq.2.2,

$$C = -\frac{1}{2\pi f Z''} \tag{2.2}$$

Where Z" is the imaginary part of the impedance frequency and f is the frequency. From the 'C' values, $1/C^2$ was calculated and was plotted against applied potential. From the slope Nd (donor defect density) and Na (acceptor defect density) can be calculated using the following equation 3.3 and 3.4, respectively:

$$\frac{1}{C^2} = \frac{2}{e\varepsilon\varepsilon_0(Nd)}\left[E - E_{FB} - \frac{kT}{e}\right] \quad \text{n-type semiconductor} \tag{2.3}$$

$$\frac{1}{C^2} = -\frac{2}{e\varepsilon\varepsilon_0(Na)}\left[E - E_{FB} - \frac{kT}{e}\right] \quad \text{p-type semiconductor} \tag{2.4}$$

where, Nd is donor defect density, Na is acceptor defect density, ε is dielectric constant of passive film, ε_0 is the permittivity of free space ($8.854*10^{-14}$ F/cm), e is the electron charge ($1.602*10^{-19}$ C), k is Boltzmann constant ($1.39*10^{-23}$ J/K), E_{FB} is flat band potential and E is applied potential.

3 RESULTS AND DISCUSSION:

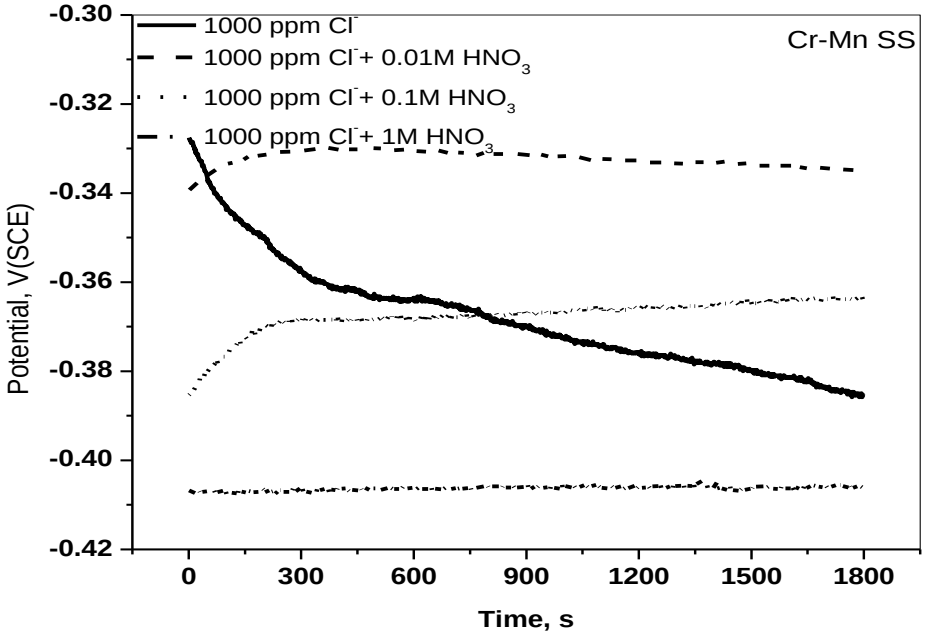

Figure 2: Effect of various concentration of HNO_3 on OCP of Cr-Mn SS in presence of 1000 ppm Cl^-.

3.1 OCP-time studies

Figure 2 shows the combined effect of HNO3 and chloride ions on OCP of Cr-Mn SS. The OCP of Cr-Mn SS in 1000 ppm Cl^- drifts from -0.33 V(SCE) to -0.385 V (SCE) at the end of 30 minutes as against -0.125 V (SCE) in DD water. This means that addition of Cl^- increases corrosion tendency of Cr-Mn SS. It is evident that on addition of 0.01M and 0.1 M HNO_3, the OCP at the end of 30 minutes shifts to noble potential and on addition 1M HNO_3 the OCP shift to a active potential of almost -0.405 V (SCE). This means that addition of 0.01M and 0.1M HNO_3 decreases tendency of Cr-Mn SS to corrode and that addition of 1M HNO_3 increases its tendency to corrode.

3.2 Potentiodynamic polarization

Figure 3 shows the effect of HNO_3 concentration in the presence of 1000 ppm Cl^- on anodic polarization of Cr-Mn SS. The plots show that cathodic parts are linear, indicating cathodic reaction to be under activation control. Further, it is evident that in bare chloride solution, active corrosion region extends up to 1 mA c.d. and then a limiting current region sets in. In all

HNO_3+Cl^- solutions the polarization plots show distinct active to passive transition with i_{pass} being more than 1µA. In all these solutions film breakdown occurs after 0.75V (SCE) and then a secondary passivity is also seen.
Table 2 presents the electrochemical parameters obtained from Figure 3.The, i_{corr} of Cr-Mn SS in 1000 ppm Cl^- solution is 3.28 µA as against 0.76 µA in distilled water. It means that the addition of 1000 ppm Cl^- has adverse effect on the steel.

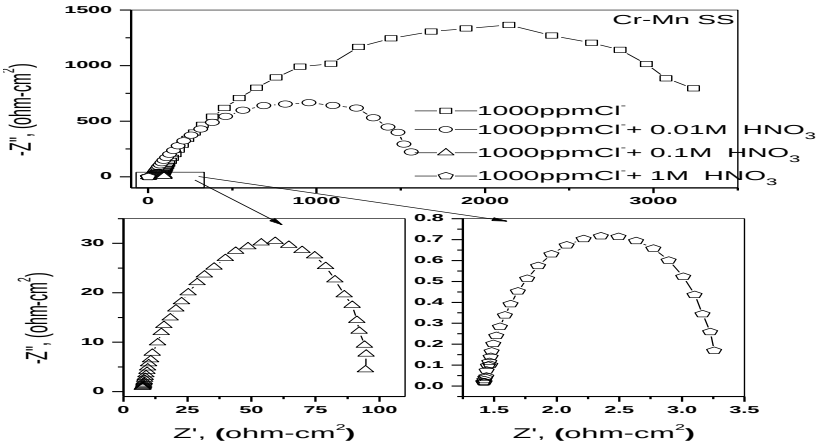

Figure 4(b): Nyquist plot of Cr-Mn SS in various concentrations of HNO_3 containing 1000 ppm Cl^-.

3.3 EIS
Figure 4 shows the effect of various concentrations of HNO_3 containing 1000 ppm Cl^- on Nyquist plot of Cr-Mn SS. It is evident that the diameter of capacitive arcs of Nyquist plots in these solutions is very low. It is evident that on increasing the concentration of HNO_3 in chloride solution, the diameter of capacitive arc of Nyquist plot decreases further. It means, film resistance decreases on addition of Cl^- and on increase in HNO_3 in chloride solution. Table 3 presents EIS fitted values of test steels measured under OCP (vs. SCE). It is evident that Rp value for Cr-Mn SS is 3.19 kohm-cm^2 in 1000 ppm Cl^- solution as against 608.5 kohm-cm^2 in DD water. The Rp values decrease further with increasing HNO_3 concentration.
For Cr-Mn SS, Cl^- and HNO_3 addition has an adverse effect. This may be attributed to the effect of pH. As pH is decreasing from 7 to 0.1 with addition of HNO_3 in chloride solution (Table 3), the film resistance is decreasing. This is attributed to thinning of passive film with drop in pH.

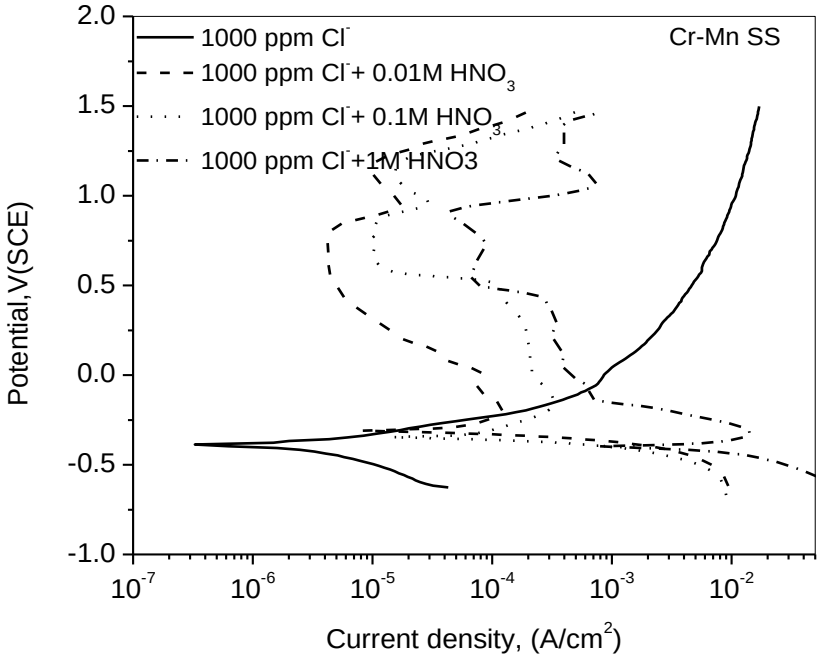

Figure. 3: Effect of various concentrations of HNO_3 on anodic polarization of

Cr-Mn SS in the presence of 1000 ppm Cl^-.

Table 2: Electrochemical parameters of test steels obtained from anodic polarization in various HNO_3 concentrations containing 1000 ppm Cl^-.

HNO_3 concentration (ppm)	1000 ppm Cl^-	0.01M HNO_3 +1000 ppm Cl^-	0.1M HNO_3 +1000 ppm Cl^-	1M HNO_3 +1000 ppm Cl^-
Type of steel (ASS)	Cr-Mn	Cr-Mn	Cr-Mn	Cr-Mn
E_{corr},V(SCE)	-0.15	-0.31	-0.34	-0.40
ßa,(mV)	112.56	1.8E7	1.3E7	3.0E7
ßc,(mV)	222.38	90.75	103.6	221.64
i_{corr}, (µA)	3.28	132.8	223.4	15.96
E_{pp}, V(SCE)	-	-0.19	-0.15	-0.32
i_{crit}, (µA)	-	122.1	325.2	14100
i_{pass}, (µA)	-	4.22	9.76	43.1
E_{pit},V(SCE)	-	0.8	0.86	0.91
E_{pit}-E_{pass}, V(SCE)	-	0.99	1.01	1.23

Table 3: EIS fitted values of test steels measured under OCP (vs. SCE) in solutions containing various HNO_3concentration containing 1000 ppm Cl^-.

HNO_3 concentration, M	Cl^- free	0.01M HNO_3 +1000 ppm Cl^-	0.1M HNO_3 +1000 ppm Cl^-	1M HNO_3 +1000 ppm Cl^-
Type of steel (ASS)	Cr-Mn	Cr-Mn	Cr-Mn	Cr-Mn
Rp, (k ohm-cm^2)	3.19	1.80	0.09	0.001
CPE-T (µF-cm^{-2})	83.47	269.7	429.33	571.2
CPE-P	0.79	0.78	0.69	0.84
Rs, (ohm-cm^2)	8.33	24.47	6.99	1.42

It is reported that a process of crevice repassivation mainly depends on the ratio of NO_3^-/Cl^- rather than on individual concentration of NO_3^- or Cl^- ions [14]. Increasing ratio of NO_3^-/Cl^- decreases passivation potential and it causes early passivation [15]. To inhibit pitting corrosion in SS, a ratio of 0.1 of NO_3^-/Cl^- is required in 10% $FeCl_3$ solution. On the other hand, a ratio of 0.067 of NO_3^-/Cl^- is adequate in 1N NaCl + 0.5HCl acidic chloride solution [14]. The ratio of 0.2 of NO_3^-/Cl^- in nitrate and chloride solution develops crevice resistance in alloy-22 [16]. Yang et al (2007) [17] have observed that the critical breakdown potential varies linearly with log $[Cl^-]$ for solution containing only Cl^- and varies with log $([Cl^-]/[NO_3^-])$ for solutions containing $Cl^-$and NO_3^- ions. It means that a particular ratio of NO_3^-/Cl^- only leads to corrosion resistance of an alloy.

3.4 Mott-Schottky analysis in HNO_3 containing 1000 ppm Cl^-

Figure 4.3 shows the M-S plots Cr-Mn SS in DD water containing 1000 ppm Cl^-. The plot for Cr-Mn SS shows two linear regions on either side of minima. These plots are similar to those reported previously for passive films on stainless steels [18]. It reflects duplex nature of the passive film; the inner chromium oxide (Cr_2O_3) region and outer iron oxide (Fe_2O_3) regions of passive films of stainless steels.

In Cr-Mn SS a negative slope is observed up till 0.347 V (SCE) and indicates a positive slope from 0.347V (SCE) to 0.86V (SCE). Potential of 0.347 V (SCE) indicates

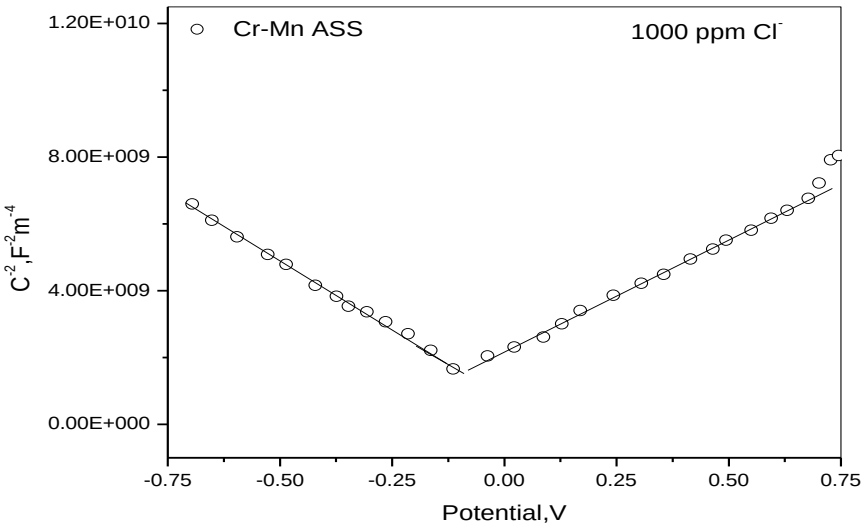

Figure 5(a): M-S plot of Cr-Mn SS in 1000 ppm Cl^- solution.

E_{FB} of Cr-Mn SS. It is evident that E_{FB} is low in Cr-Mn SS. It is likely that lower E_{FB} would yield higher pitting potential [6]. It is evident that in the region of negative slope, the plot of Cr-Mn SS. It means that values of $1/C^2$ for Cr-Mn SS are higher. According to finding of Hakiki et al [18], slope of negative plot in M-S plots of Fe-Cr alloys, decreases with increasing Cr content. In the region of positive slope, the plot of Cr-Mn SS lies above. It is evident that the slope Cr-Mn SS is low.It is evident that the positive slope of Cr-Mn SS is low. This is in agreement with the findings of Hakiki et al [18] that defect density increases with decreasing Cr content of Fe-Cr alloys and that the effect is more clearly seen in negative slope part of M-S plot. This indicates that Cr-Mn SS has more oxygen vacancy in the film.

Less resistant film should have more cation vacancies; this is what has been found in M-S studies. For Cr-Mn SS, Na increases from 12.6 $x10^{20}cm^{-3}$ (in 1000 ppm Cl^-) to 87.5 $x10^{20}cm^{-3}$ on addition of 0.1M HNO_3. No doubt that it increases corrosion rate as has been found for the test steels.

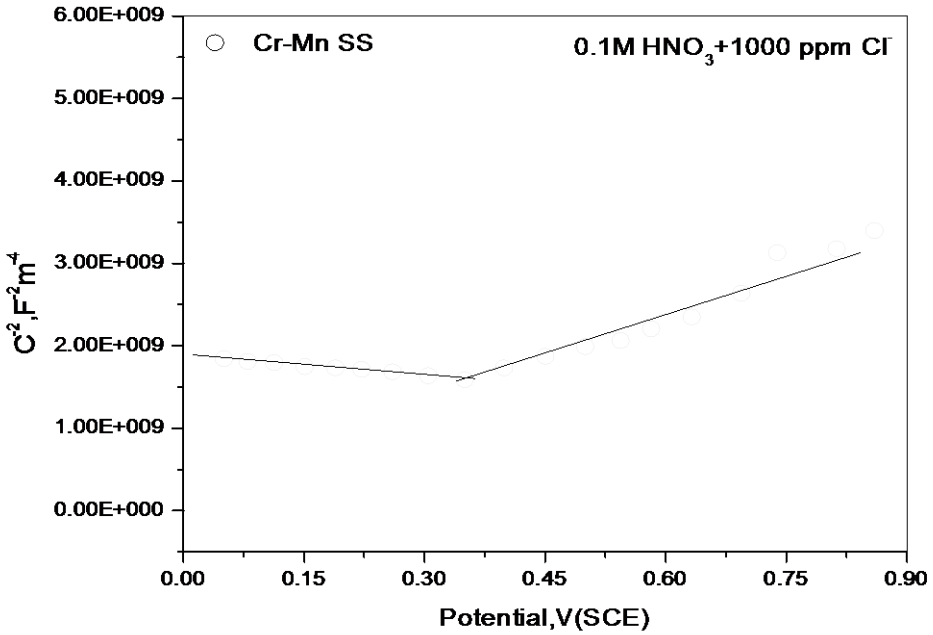

Figure 5(b): M-S plot of 304 SS and Cr-Mn SS in 0.1M HNO_3+1000 ppm Cl^- solution.

Table 4: Defect density of test steels in various solutions ($10^{20}/cm^3$)		
Solution	Cr-Mn SS	
	Na	Nd
Distilled water +1000 ppm Cl^-	12.6	13.7
0.1M HNO_3 + 1000 ppm Cl^-	87.5	29.6

4 CONCLUSIONS:

(1) It was found that density of the cation vacancies in the film forming on Cr-Mn ASS in 1000 ppm Cl^- solution was 12.6 $x10^{20}$ per cm^3, and increased to 87.5 $x10^{20}$ per cm^3 on addition of HNO_3.

(2) From EIS results it was found that polarisation resistance (Rp) decreased on addition of HNO_3 Cr-Mn ASS. This is attributed to effect of pH on stability of Cr_2O_3 film.

(3) Addition of 0.01M and 0.1M HNO_3 decreases tendency of Cr-Mn SS to corrode and that addition of 1M HNO_3 increases its tendency to corrode.

(4) The i_{corr} of Cr-Mn SS in 1000 ppm Cl^- solution is 3.28 µA as against 0.76 µA in distilled water. It means that the addition of 1000 ppm Cl^- has adverse effect on both the steels.

5. REFERENCES:

[1] A. J. Sedrik, Corrosion of Stainless Steels, 2 nd ed., John Wiley & Sons, New York. 1996.

[2] T. Oshima, Y. Habara, and K. Kuroda, "Efforts to Save Nickel in Austenitic Stainless Steels," ISIJ International, vol. 47, no. 3, pp. 359–364, 2007.

[3] ISSF, Brussels, "' New 200-series ' steels : An opportunity or a threat to the image of stainless steel," November, 2005.

[4] P. C. Pistorius and M. Toit, "LOW-NICKEL AUSTENITIC STAINLESS STEELS : METALLURGICAL CONSTRAINTS," in The Twelth International Ferroalloys Congress; Sustainable Future, 2010, pp. 911–918.

[5] C. Abreu, M. Cristobal, R. Losada, X. Novoa, G. Pena, and M. Perez, "The effect of Ni in the electrochemical properties of oxide layers grown on stainless steels," Electrochimica Acta, vol. 51, no. 15, pp. 2991–3000, Apr. 2006.

[6] S. Ningshen, U. Kamachimudali, V. Mittal, and H. Khatak, "Semiconducting and passive film properties of nitrogen-containing type 316LN stainless steels," Corrosion Science, vol. 49, no. 2, pp. 481–496, Feb. 2007.

[7] H. P. Leckie and H. H. .Uhlig, "Environmental Factors Affecting the Critical Potential for Pitting in 18–8 Stainless Steel 1.," J. Electrochem. Soc., vol. 113, no. 12, pp. 1262–1267, 1966.

[8] K. Sugimoto and Y. Sawada, "The role of molybdenum additions to austenitic stainless steels in the inhibition of pitting in acid chloride solutions," Corrosion Science, vol. 17, pp. 425–445, 1977.

[9] H. El Dahan, "Pitting corrosion inhibition of 316 stainless steel in phosphoric acid-chloride solutions Part II AES investigation," Journal of materials science, vol. 4, pp. 859–868, 1999.

[10] S. Maximovitch, G. Barral, F. Le Cras, and F. Claudet, "The electrochemical incorporation of molybdenum in the passive layer of a 17% Cr ferritic stainless steel. Its influence on film stability in sulphuric acid and on pitting corrosion in chloride media," Corrosion Science, vol. 37, no. 2, pp. 271–291, Feb. 1995.

[11] D. Kim, Clayton C.R. and O. M., "On the question of nitrate formation by N-containing austenitic stainless steels," Materials Science and Engineering A, vol. A186, pp. 163–169, 1994.

[12] S. Ramya, T. Anita, H. Shaikh, and R. K. Dayal, "Laser Raman microscopic studies of passive films formed on type 316LN stainless steels during pitting in chloride solution," Corrosion Science, vol. 52, no. 6, pp. 2114–2121, Jun. 2010.

[13] F. M. Bayoumi and W. A. Ghanem, "Effect of nitrogen on the corrosion behavior of austenitic stainless steel in chloride solutions," vol. 59, pp. 3311–3314, 2005.

[14] G. O. Ilevbare, K. J. King, S. R. Gordon, H. a. Elayat, G. E. Gdowski, and T. S. E. Gdowski, "Effect of Nitrate on the Repassivation Potential of Alloy 22 in Chloride-Containing Environments," Journal of The Electrochemical Society, vol. 152, no. 12, p. B547, 2005.

[15] R. C. Newman and M. A. A. Ajjawi, "A micro-electrode study of the nitrate on pitting of stainless steels," Corrosion Science, vol. 26, no. 12, pp. 1057–1063, 1986.

[16] A. K. Mishra and G. S. Frankel, "Crevice Corrosion Repassivation of Alloy 22 in Aggressive Environments," Corosion, vol. 64, no. 11, pp. 836–844, 2008.

[17] D. D. Macdonald, Shoufeng Yang, "Theoretical and experimental studies of the pitting of type 316L stainless steel in borate buffer solution containing nitrate ion," Electrochimica Acta, vol. 52, pp. 1871–1879, 2007.

[18] N. E. Hakiki, B. Rondot, and S. Boudin, "The electronic formed structure of passive films on stainless steels," Corrosion, vol. 37, no. 11, pp. 1809–1822, 1995.